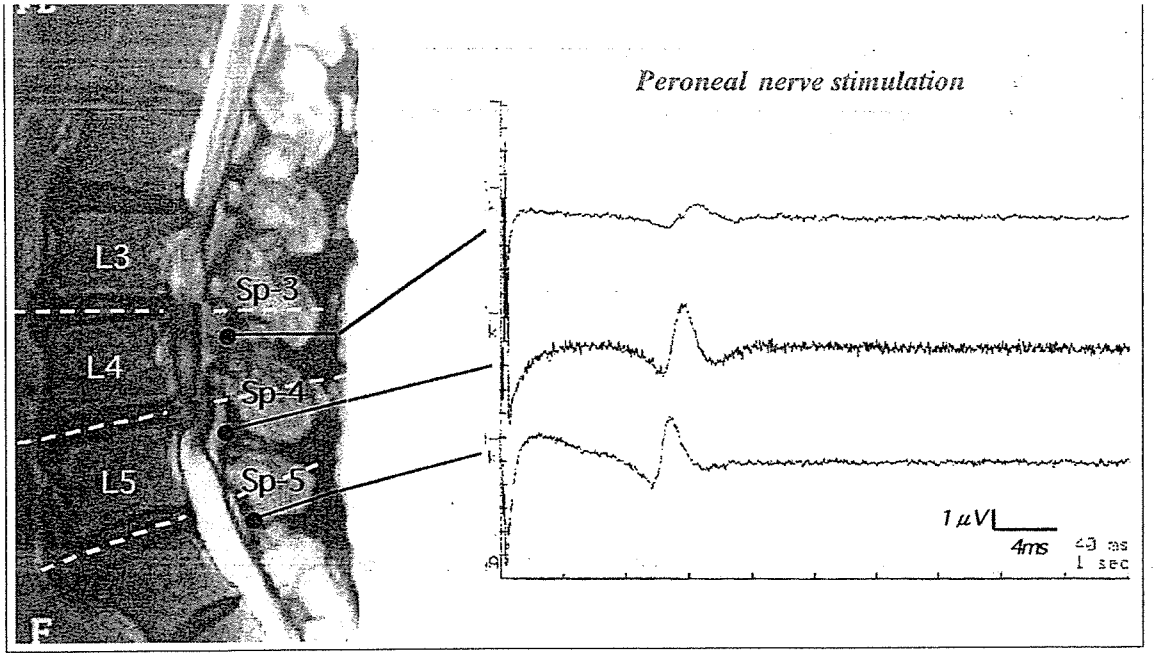

図 8.
第 5 腰髄神経根障害例の CEAP
67 歳，男性(図 1 と同一症例)．脛骨神経刺激，腓骨神経刺激の CEAP は両者とも L 3-4 で振幅の低下と波形の変化を認めた．図の中の，Sp-5 は第 5 腰椎棘突起を表している．電極は棘突起間レベルの椎弓間の黄色靱帯に設置し単極誘導記録していることから，椎間板レベルより尾側に記録電極は設置される．したがって，L 4-5 → L 3-4 における振幅の低下は L 4-5 椎間板レベルでの狭窄が関与していると考えられる．L 4-5 の除圧を行い症状は改善した．

(24.5%)であった．また，腓骨神経刺激-CEAP の control 波形の振幅は，L 4-5 記録で振幅が最大となる症例が 45 例中 28 例(62.2%)，L 34 記録で振幅が最大となる症例が 45 例中 17 例(37.8%)であった[19]．理論的には，刺激部位から遠ざかる(頭側に向かう)ほど潜時は延長し振幅は小さくなるのが普通であるが，腓骨神経刺激(脛骨神経)-CEAP の振幅は L 4-5(L 5-S 1)で記録される誘発電位よりも L 3-4(L 4-5)で記録される誘発電位の方が大きい症例も存在した．これは，脛骨神経や腓骨神経が複数の神経根に由来する線維で構成されていることが理由と考えられ，波形解析の際には留意する必要がある(図 4)．

従来の方法で CEAP を記録する場合，明らかな異常波形の検出率は必ずしも高くない．その理由の第 1 は腓骨神経が L 4, L 5, S 1, S 2 根から，脛骨神経が L 4, L 5, S 1, S 2, S 3 根からというようにともに多くの神経根からの線維を含んでおり，そのために障害神経根の異常電位は他の神経根由来の正常電位によって隠蔽され，単根障害では波形異常を呈しにくいと考えられる．理由の第 2 は，LSCS における間欠跛行に象徴されるように腰椎や神経に負荷が加重された時のみに伝導ブロックや伝導遅延が生じ，安静時にはそれらが正常化することが多いためではないかと考えられる．

9．複数椎間狭窄を伴う腰部脊柱管狭窄症症例の責任高位決定のプロセス

1）画像上の異常椎間高位の把握

責任高位決定のプロセスに入る前に，まず神経学的所見を詳細に診察することが重要である．間欠性跛行を伴う腰部脊柱管狭窄症症例では，歩行することで知覚障害レベル，筋力，反射所見などが変化する場合もあるので，歩行前後の神経学的所見をとることも必要である．続いて，脊髄造影，CTM, MRI などの画像検査を施行し画像上の異常椎間高位を把握する．

2）障害神経根の把握

神経学的所見と画像所見から障害神経根を推定し，針筋電図や神経根ブロックなどの機能的検査を行い障害神経根を同定する．下肢痛を有する症例に対しては，神経根ブロックを行い下肢痛の消失を認めれば障害神経根と判断できる．下肢痛のない症例では神経根ブロックはあまり有用ではない．以上のプロセスから単一神経根障害か複数神経根障害かを判断する．解剖学的には，脊柱管の各椎間でその椎間から分岐する神経根は脊柱管の最外側に位置しており，その椎間より末梢で分岐する脊髄神経はその内側に存在する[20]．したがって，当該椎間で分岐する神経根障害を伴わずに下

位レベルで分岐する神経根が障害されるとは考えにくいことから，単一神経根障害の場合は神経根の分岐するレベルでの障害の可能性が高い．複数神経根障害例では，単一椎間高位での障害として矛盾しないかどうかの判断が必要となる．最上位の障害神経根が分岐するレベルより頭側の狭窄高位は責任高位から除外できるが，それより尾側で認める狭窄高位は除外できない．

3）伝導障害高位の判定と除圧レベルの決定

術前評価をふまえて手術中に馬尾神経活動電位(CEAP)を記録し伝導障害高位を判定し，症状の発現に関与しないレベルを可能な限り除外し除圧範囲を決めている[17)18)]．2）の段階で除外できなかった高位のうち，CEAPの多相化や潜時の遅延，振幅の減少，陽性波の振幅増大現象などの所見が認められる最も尾側のレベルを責任高位の最下端とすることができる．もし，術中電気診断以前のステップで絞り込んだ責任高位の最頭側(A)と電気診断で異常所見を認めた最尾側のレベル(B)が一致すれば除圧範囲を1椎間に絞ることができる．しかし，一致しない場合には(A)と(B)に挟まれる椎間を全て除圧することになる．

10．他科領域の疾患と腰仙部神経根障害との鑑別

臨床の現場では他科的疾患との鑑別に難渋する症例に少なからず遭遇する．たとえば，麻痺性下垂足の鑑別診断として総腓骨神経麻痺，第5腰髄神経根障害(圧迫性神経根障害，脱髄性疾患など)，ポリオ，脳血管障害などが考えられるが，MRIなどの画像検査で捉えることができるのは脳血管障害や圧迫性神経根障害であり，末梢神経障害，ALSなどの神経変性疾患や神経根を中心に脱髄病変を呈するCIDPを画像で捉えることは困難な場合が多い．このような場合には，電気生理学的検査で神経伝導路の障害の有無や神経軸索機能を客観的かつ機能的に評価し診断できる場合も少なくない．たとえば，針筋電図検査でpositive sharp waveが前脛骨筋に認められれば脊髄前角部～馬尾～末梢神経の経路のどこかで軸索変性を伴う病変が存在すると診断できるし，F波の出現率の減少や潜時に遅延が認められれば脊髄前角部～馬尾～末梢神経の経路のどこかで伝導障害を生じさせる病変が存在すると診断できる．また，M波やSNAPのconduction studyを行って伝導速度の低下や潜時の遅延を認めれば，神経根を含めた末梢神経障害と診断することができる．これらの電気生理学的検査に加えてSEPで脊髄伝導路系に異常を捉えることができない場合には，脳血管障害などの中枢神経の異常を考える必要がある．

では，M波，SNAP，F波などの電気生理学的検査で異常を認めた場合には前角部～末梢神経の経路のどこかで必ず病変があると判断できるのであろうか？　原則的にはそのように判断できるが，我々は上肢の麻痺が転換性障害(いわゆるヒステリー)に代表される精神的疾患に起因すると考えられるにもかかわらずM波，SNAP，F波，MEPなどの電気生理学的検査で異常所見をしめした症例を経験している．

症　例：27歳，女性(図6，7)．右上肢麻痺

病院を転々として原因不明といわれ，発症後3か月で来院した．MMTは，左上肢は正常であるのに対し右上肢は三角筋，右上腕二頭筋，右上腕三頭筋は3～3－であり，握力も左26.5 kg，右6.5 kgと右優位の筋力低下を認めた．また，右上肢に感覚障害を認めるのに対し，左上肢の感覚異常は認めなかった．上下肢の深部腱反射はすべて正常で，病的反射は認めなかった．M波(正中神経刺激-短母指外転筋記録)，正中神経SNAP，MEP，F波では左右差を認め，健側と比べて患側の右側で導出された誘発電位の振幅は小さくF波の出現率は低かった(図7)．しかし，運動障害・感覚障害を説明しうる画像所見(図6)・生化学検査などに異常を指摘することができず，運動麻痺の程度に矛盾する動作がみられたことから転換性障害(ヒステリー)と診断された．この症例は，運動障害の原因となったと思われる因子が暴露されなく

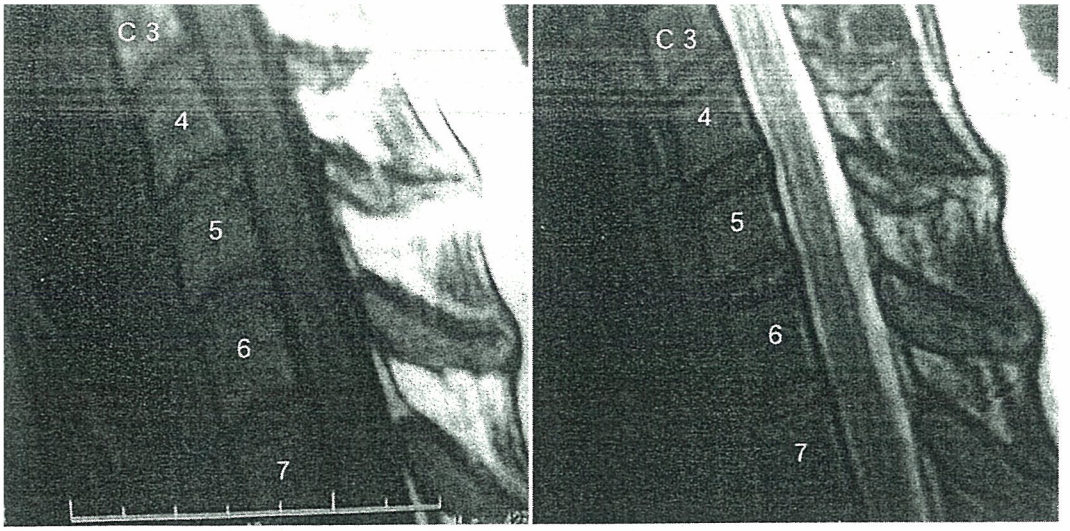

a | b

図 6.
転換性障害(ヒステリー)による右上肢麻痺例の MRI 画像
27 歳，女性．椎間板ヘルニアや脊柱管狭窄症などの圧迫性脊髄病変を認めない．
a：T 1
b：T 2

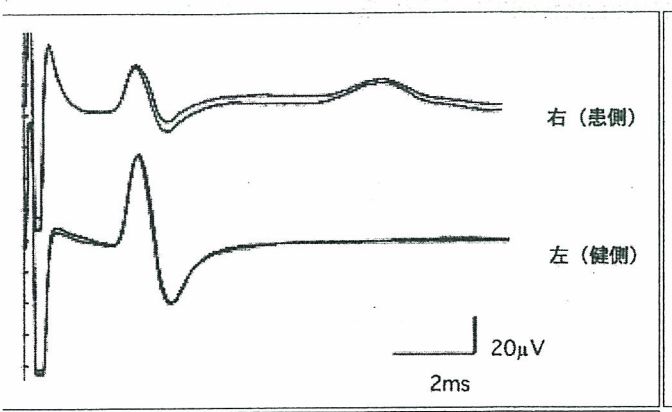

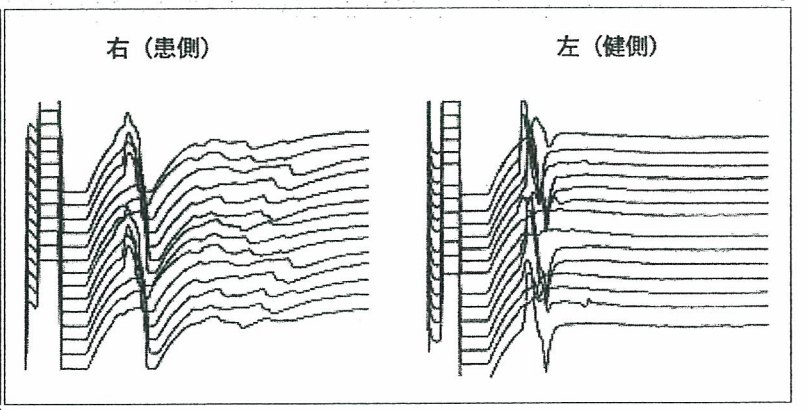

a | b
c |

図 7.
転換性障害(ヒステリー)による右上肢麻痺例の各種誘発電位
27 歳，女性(図 6 と同一症例)．正中神経の SNAP の振幅は健側(左)に比して患側(右)の方が小さい．また，短母指外転筋で記録した F 波の出現率は右 89.3%，左 92.9%で，平均振幅は右 0.332 mV，左 0.426 mV($p<0.04$)と患側の方が小さい．短母指外転筋の MEP でも右(患側)の方が振幅が小さい．
a：正中神経 SNAP
b：F 波(正中神経刺激-短母指外転筋記録)
c：MEP(経頭蓋磁気刺激-短母指外転筋記録)

なった後は症状の消失をみている．

このように運動麻痺として身体症状が表現された場合，結果的に四肢を動かしていないという状態がある一定の時間持続することとなる．淵上ら[21]は，意識的か否かにかかわらず，持続的な脱力のある場合には前角細胞の興奮性，つまり運動ニューロンの興奮性が低下し MEP の振幅が減少することが報告されており，同様な機序で F 波の振幅も低下するものと推察される．M 波・SNAP の振幅低は，intertrial variability である可能性，利き手側の SNAP の振幅が非利き手側より小さいケースである可能性や[22]，長時間の不動化により神経・筋の興奮性が低下した可能性が考えられた[23]．このように何らかの理由で不動の状態が続いた場合には M 波，F 波，SNAP，MEP などの電気生理学的検査で左右差を示す場合があることに留意し，下肢の麻痺を生じた症例においても同様な可能性を念頭におく必要がある．

文 献

1) Wilbourn, A. J., et al. : AAEM Minimonograph # 32 : The electrophysiologic examination in patients with radiculopathies. Muscle Nerve. **11** : 1099-1114, 1988.
2) Phillips II, L. H., et al. : Electrophysiologic mapping of the segmental anatomy of the muscles of the lower extremity. Muscle Nerve. **14** : 1213-1218, 1991.
3) Kimura, J. : Electrodiagnosis in Disease of Nerve and Muscles ; Principles and Practice (2 nd ed.). FA Davis. 55-102, 1989.
4) Tani, T., et al. : Electrophysiologic assessment of shoulder girdle weakness in patients with cervical sponsylosis : Prognostic value of supraclavicular stimulation. J Clin Neuromus Dis. **4** : 11-18, 2002.
5) Jabre, J. F. : The superficial peroneal sensory nerve revisited. Arch Neurol. **38** : 666-667, 1981.
6) LaFratta, C. W., et al. : Age effects on sural nerve conduction velocity. Arch Phys Med Rehabil. **54** : 475-477, 1973.
7) Schuchmann, J. A. : Sural nerve conduction ; a standardized technique. Arch Phys Med Rehabil. **58** : 166-168, 1977.
8) 谷 俊一 : 腰部脊柱管狭窄症の機能診断. 整・災外. **34** : 261-270, 1991.
9) 谷 俊一ほか : 腰仙部馬尾・神経根障害における下肢末梢知覚神経誘発電位測定とその意義について. 中部整災誌. **32** : 1379-1381, 1989.
10) 石田健司ほか : 腰部脊柱管狭窄症に伴う間歇性跛行に関する検討—姿勢動揺と電気生理学的評価を指標として. 日脊会誌. **6** : 324, 1995.
11) Scott, F., et al. : Dynamic F wave in neurogenic claudication. Muscle Nerve. **14** : 457-461, 1991.
12) Barker, A. T., et al. : Noninvasive magnetic stimulation of human motor cortex. Lancet. **1** : 1106-1107, 1985.
13) Dvorak, J. et al. : Magnetic stimulation of motor cortex and motor roots for painless evaluation of central and proximal peripheral motor pathways. Spine. **16** : 995-961, 1991.
14) Ishida, K., et al. : Recovery of spinal cord conduction after surgical decompression for cervical spondylotic myelopathy : serial somatosensory evoked potential studies. Am J Phys Med Rehabil. **82** : 130-136, 2003.
15) 松田英雄ほか : 電気診断. 整形災害外科別冊. 腰痛—その診断と治療のすべて. 蓮江光男, 鈴木勝己, 山内裕雄編. 92-106, 金原出版, 1983.
16) 谷 俊一ほか : 腰椎椎間板ヘルニアの電気生理学的診断法. MB Orthop. **2** : 27-37, 1988.
17) 谷口愼一郎ほか : 腰部脊柱管狭窄症に対する除圧レベル決定に関する検討. 骨・関節・靱帯. **9** : 1359-1369, 1996.
18) Taniguchi, S. : Mini-symposium. Lumbar spinal canal stenosis (iii) Decompression surgery for lumbar canal stenosis. Current Orthopaedics. **13** : 184-190, 1999.
19) 谷口愼一郎ほか : 電気診断法. 整形外科 NEW MOOK 9 腰部脊柱管狭窄(症), 越智隆弘/菊地臣一編. pp 110-120, 金原出版, 2001.
20) Wall, E. J., Cohen, M. S., Massie, J. B., et al. : Cauda Equina Anatomy I ; Intrathecal Nerve Root Organization. Spine. **15** : 1244-1247, 1990.
21) 淵上泰敬ほか : 磁気刺激運動誘発電位に対する持続的脱力の影響. 脊髄電気診断学. **16** : 82-85, 1994.
22) Martinez, A. C., et al. : Ratio between the amplitude of sensory evoked potentials at the wrist in both hands of left-handed subjects. J Neurol Neurosurg Psychiatry. **43** : 182-184, 1980.
23) McComas, A.J., et al. : Distal dysfunction and recovery in ulnar neuropathy. Muscle Nerve. **19** : 1617-1619, 1996.

腰仙部神経根障害に対する後方手術時に記録した馬尾神経活動電位の検討

川田倫子[1)]、谷口愼一郎[1)]、石田健司[2)]、牛田享宏[1)]、
岸本裕樹[1)]、池本竜則[1)]、 谷 俊一[1)]

高知大学医学部整形外科[1)]
高知大学医学部リハビリテーション部[2)]

Analysis of cauda equina action potentials recorded from the ligamentum flavum after peroneal nerve and tibial nerve stimulation at the knee during surgery for lumbosacral radiculopathies

Tomoko Kawada[1)], Shinichirou Taniguchi[1)], Kenji Ishida[2)], Takahiro Ushida[1)], Hiroki Kishimoto[1)], Tatsunori Ikemoto[1)], Toshikazu Tani[1)]

Department of Orthopaedic Surgery, Kochi Medical School[1)]
Rehabilitation center, Kochi Medical School Hospital[2)]

Key Words : cauda equina action potential, lumbar disc herniation , electrodiagnosis

Abstract

We studied the cauda equina action potentials (CEAPs) recorded intraoperatively, with active needle electrodes placed into the ligamentum flavum in the midline at serial lumbar levels and a common reference electrode inserted into the skin rostrally to the operative site and contralaterally to the side of stimulation, after unilateral stimulation of the peroneal nerve or the tibial nerve at the knee. When evoked by stimulation on the asymptomatic side in 33 patients with unilateral radiculopathies, the peroneal- and the tibial-CEAPs (mean ± SD) increased in onset latency progressively toward the rostral level with the latency differences between two adjacent levels of 0.33 ± 0.03 ms and 0.35 ± 0.12 ms for L 4-5/L 5-S 1 and 0.47 ± 0.16 ms and 0.47 ± 0.15 ms for L 3-4/L 4-5, respectively. The amplitudes of the peroneal-CEAPs were 127 ± 28 % at L 4-5, 121 ± 39% at L 3-4 and 116 ± 51% at L 2-3 compared to the L 5-S 1 level, which were measured from the baseline. The corresponding values (% ampli-

tude) for the tibial-CEAP were 95±22% at L 4-5 , 91±29% at L 3-4 and 82±35 % at L 2-3.
When tested on the 14 patients with a distinct disc herniation by stimulating the symptomatic side, the peroneal-CEAPs revealed focal conduction abnormalities across the lesion site in 11 patients (79%) and the tibial-CEAPs in 12 (86%), as evidenced by the latency difference between two adjacent levels and/or the % amplitude being outside the mean±2 SD in the data on 33 asymptomatic limbs.

はじめに

我々は腰椎後方手術時に膝窩部で腓骨神経あるいは脛骨神経を刺激し、各椎弓間部の黄色靭帯に設置した針電極から単極誘導にて馬尾神経活動電位（以下、CEAP）[1,2,3,4,5]を記録してきた。今回、CEAPの正常波形を分析するために、下肢症状が一側のみの患者で記録したCEAPのうち無症状側のCEAPの潜時や振幅を検討し、このデータから腰椎椎間板ヘルニア症例のCEAPの異常を診断できるか否か検討したので報告する。

対象および方法

1. 記録方法

Dantec社製Evomatic 8000筋電計を用いて記録した。腓骨神経及び脛骨神経は膝窩部で最大上刺激し、記録は黄色靭帯正中部でL2-3～L5-S1に刺入した単極針電極から100回加算平均した。Fig.1に示す方法で潜時と振幅を各椎弓間レベルで計測した。振幅については、各症例ごとにL5-S1の振幅に対する割合を計算し平均値を求めた。

2. 無症状側CEAPの検討

対象は腰仙部神経根障害症例で手術を施行し、手術中にCEAPを記録した患者のうち下肢症状が一側のみに認められた33症例であり、疾患の内訳は、腰椎椎間板ヘルニア13例、腰椎分離症13例、腰部脊柱管狭窄症5例、腰椎分離すべり症2例であり、年齢は平均45歳であった。これらの症例で手術中に記録したCEAPのうち無症状側のCEAPの潜時および振幅を計測し、身長や年齢と潜時との相関を検討した。

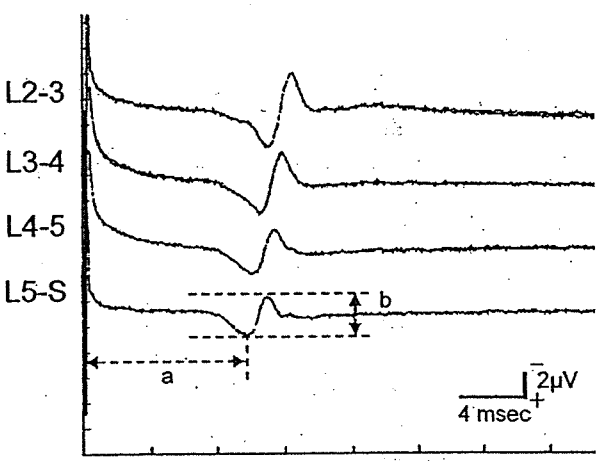

Fig.1 CEAPs recorded after stimulating peroneal nerve at popliteal fossa of the asymptomatic lower leg. As labeled in the bottom tracing, the latencies were measured to the onset of the major potentials (a) and the amplitudes were measured from the positive peak to the negative peak of the major potentials (b).

3. 腰椎椎間板ヘルニアCEAPの検討

無症状側CEAPのデータを参考に、腰椎椎間板ヘルニア症例のCEAPで電気生理学的な異常を診断できるかどうか検討した。対象は腰椎椎間板ヘルニア22症例であり、ヘルニアのレベルはL4-5レベルが14例、L5-S1レベルが8例であり、年齢は平均48歳であった。異常の判定は、無症状側のCEAPで得られた潜時あるいは潜時差のmean+2 SD、振幅のmean±2 SDをcut off値としてこの値を超える場合を異常として判定した。

Table 1.　Onset latency of peroneal-CEAPs and tibial-CEAPs

	peroneal-CEAPs Mean±SD(ms)	P-value	tibial-CEAPs Mean±SD(ms)	P-value
L2-3	10.8±1.7		10.7±1.9	
L3-4	10.5±1.8	P>0.05	10.2±1.9	P>0.05
L4-5	10.0±1.7	P<0.01	9.7±1.8	P<0.01
L5-S1	9.7±1.6	P<0.01	9.4±1.8	P<0.01

Table 2.　% Amplitude of peroneal-CEAPs and tibial-CEAPs

The amplitudes were expressed as % amplitude, which were defined as a percentage relatively to those at L 5-S 1.

	peroneal-CEAPs Mean±SD(%)	P-value	tibial-CEAPs Mean±SD(%)	P-value
L2-3	116.0±51.3	P<0.01	82.0±34.7	P<0.01
L3-4	120.5±39.1	P<0.01	91.0±28.6	P<0.01
L4-5	126.6±28.0	P<0.01	94.9±22.0	P<0.01
L5-S1	100		100	

The amplitudes were expressed as %amplitude, which were defined as a percentage relatively to those at L5-S1.

Table 3.　Latency difference between two adjacent levels of peroneal-CEAPs and tibial-CEAPs

	peroneal-CEAP Mean ± SD(ms)	tibial-CEAPs Mean ± SD (ms)
L3-4/4-5	0.47±0.16	0.47±0.15
L4-5/5-S1	0.33±0.13	0.35±0.12

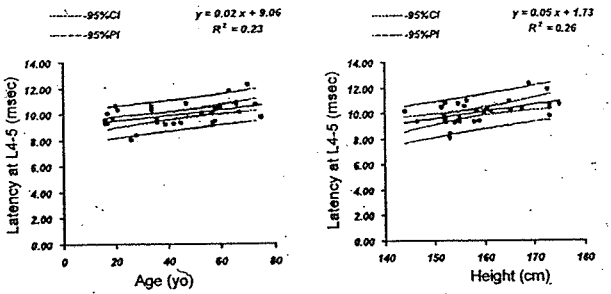

Fig.2　Correlation between age/height and latency in peroneal-CEAPs

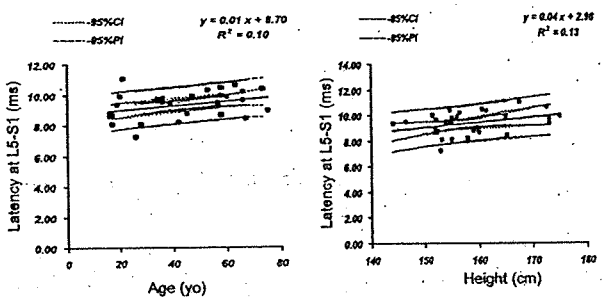

Fig.3　Correlation between age/height and latency in tibial-CEAPs

結果

1. 無症状側 CEAP の検討

無症状側の腓骨神経あるいは脛骨神経を刺激して得られた CEAP（脛骨神経 CEAP、腓骨神経 CEAP）の潜時は、頭側に向かうに従って潜時が延長していた（Table 1）。腓骨神経 CEAP の振幅は、L 4-5 で最も大きく、L 4-5 より頭側に向かうに従って振幅は小さくなっていた。一方、脛骨神経 CEAP の振幅は L 5-S 1 で最も大きく頭側に向かうに従って振幅は小さくなっていた（Table 2）隣接する椎弓間の潜時から計算した潜時差の平均値と標準偏差は Table 3 に示す。

また、腓骨神経及び脛骨神経 CEAP において、潜時と年齢、潜時と身長の相関は非常に弱かった（Fig.2, Fig.3）。

2. 腰椎椎間板ヘルニア CEAP の検討

(1) L 4-5 椎間板ヘルニア症例（Table 4）

L 4/5 腰椎椎間板ヘルニア症例で、潜時から伝導異常が判断できたのは、腓骨神経 CEAP では 14 例中 3 例 21% であり、脛骨神経 CEAP では 14 例中 3 例 21% であった。

振幅から伝導異常が判断できたのは、腓骨神経 CEAP では 14 例中 6 例 43% であり、脛骨神経 CEAP では 14 例中 5 例 36% であった。

潜時差を用いて伝導異常が診断できたのは、腓骨神経 CEAP では 14 例中 11 例 79% であり、脛骨神経 CEAP では 14 例中 12 例 86% であった。

(2) L 5-S 1 椎間板ヘルニア症例（Table 5）

L 5-S 1 腰椎椎間板ヘルニア症例で、潜時から伝

Table 4. Factors and their sensitivities to diagnose the conduction abnormalities in patients with L 4–5 lumbar disc herniation

		latency	amplitude		latency difference
peroneal-CEAPs	L3-4	1	2	L3-4/4-5	7
	L4-5	2	4	L4-5/5-S	4
	L5-S1	0	0		
	sensitivity	21%	43%		79%
		latency	amplitude		latency difference
tibial-CEAPs	L3-4	1	3	L3-4/4-5	8
	L4-5	2	2	L4-5/5-S	4
	L5-S1	0	0		
	sensitivity	21%	36%		86%

Table 5. Factors and their sensitivities to diagnose the conduction abnormalities in patients with L 5–S 1 lumbar disc herniation

		latency	amplitude
peroneal-CEAPs	L3-4	0	0
	L4-5	1	5
	L5-S1	2	0
	sensitivity	43%	71%
		latency	amplitude
tibial-CEAPs	L3-4	0	0
	L4-5	0	3
	L5-S1	1	0
	sensitivity	13%	38%

導異常が判断できたのは、腓骨神経 CEAP では 7 例中 3 例 43% であり、脛骨神経刺激 CEAP では 8 例中 1 例 13% であった。
振幅から伝導異常が判断できたのは、腓骨神経 CEAP で 7 例中 5 例 71% であり、脛骨神経 CEAP では 8 例中 3 例 38% であった。

考察

無症状側の潜時及び振幅の平均値から判定した腰椎椎間板ヘルニア症例の CEAP の異常の診断率はきわめて低く、不満足な結果であった。その理由を考察すると、①潜時や振幅は年齢や身長などの因子に影響をうけやすいので、これらの因子を考慮せずに単純に raw data を平均しただけでは診断の精度が上がらない、②症例の母数が少なく、年齢や身長で補正するために十分な症例でなかった、などが考えられる。
そこで、我々は各椎間の潜時差を求めることで異常を判定できないか検討した。潜時差の場合、年齢や身長の影響を回避しやすいと考えられるので、腰椎椎間板ヘルニア症例における電気生理学的異常所見の診断率を検討した。潜時差のデータを用いて異常を判定し、潜時の遅延を客観的に評価すると、L 4-5 腰椎椎間板ヘルニア症例における診断率は約 80% であり比較的満足しうる結果が得られた。潜時差と振幅から異常と判定すると診断率は 90% とさらに診断精度は上昇する。潜時差から診断する方法は、L 4–5 椎間障害の診断法として成り得ると考えられた。しかし、S 1-2 間で電位を記録していないので L 5-S 1/S 1-2 間の潜時差を計算できず、L 5-S 1 レベルの診断法としては不十分であることが問題点としてあげることができる。

文献

1. 松田英雄、近藤正樹、林俊一、他：電気診断. 整形災害外科別冊、腰痛 - その診断と治療のすべて、蓮江光男、鈴木勝己、山内裕雄編、金原出版、pp 92–106、1983.
2. 藤田泰宏、山本博司、谷俊一、他：腰仙部根症状の発症に関する電気生理学的考察. 臨整外 22 : 387–391、1987.
3. 谷俊一、木田和伸、安藤正明、他：腰部脊柱管狭窄症の機能診断. 整形災外科 34 : 261–270、1991.
4. 谷口愼一郎、谷俊一、石田健司、他：特集・腰部脊柱管狭窄症　電気診断法、NEW MOOK 整形外科 9、越智隆弘、菊地臣一(著)、110–120、金原出版、東京、2001.
5. Taniguchi S, Tani T, Ushida T, et al. : A sensitive electrodiagnostic method for detecting sensory conduction deficits in an experimental single lumbar radicular lesion. Spine 27 : E 139–144, 2002. (IF : 1.853)

Effect of Serum Albumin on QRS Wave Amplitude in Patients Free of Heart Disease

Yoshihiro Kudo, MD, Fumiyasu Yamasaki, MD, Hiromi Kataoka, MS, Yoshinori Doi, MD, and Tetsuro Sugiura, MD

We studied 193 patients free of heart disease to determine the relation between QRS amplitude and serum albumin. Although there were no significant differences in echocardiographic indexes between the 2 groups, albumin (35.1 ± 4.3 vs 40.1 ± 3.2 g/L) and colloid osmotic pressure (21 ± 4 vs 24 ± 3 mm Hg) were significantly lower in patients with low voltages compared with those without. Moreover, there was a good relation (r = 0.78) between change in QRS amplitude and change in albumin concentration. ©2005 by Excerpta Medica Inc.

(Am J Cardiol 2005;95:789–791)

Low voltage is 1 of the electrocardiographic manifestations in patients with pericardial effusion,[1–4] but it is also found in other disorders, including myocardial disease, lung disease, hypothyroidism, and obesity. [5] Serum albumin has been reported to have a direct correlation with QRS amplitude[6]; other investigators found an inverse relation between QRS amplitude and body weight in patients with anasarca.[7] However, as anasarca is frequently associated with decreased albumin concentration, the particular effect of albumin in modulating electrocardiographic voltage is yet to be defined. Accordingly, we designed a study to determine the effect of albumin concentration on QRS wave amplitude in patients free of heart and lung diseases.

• • •

Among 5,766 consecutive patients who were referred to our echocardiography laboratory between January 1, 1998, and December 31, 2001, we investigated 193 clinically stable patients (aged 41 to 95 years) with no history of heart or lung disease and no electrocardiographic, chest radiographic, or echocar-

From the Departments of Laboratory Medicine and Medicine and Geriatrics, Kochi Medical School, Kochi, Japan. Dr. Sugiura's address is: Department of Laboratory Medicine, Kochi Medical School, Kohasu Oko-cho Nankoku City, Kochi 783-8505, Japan. E-mail: sugiurat@med.kochi-u.ac.jp. Manuscript received August 30, 2004; revised manuscript received and accepted November 18, 2004.

0002-9149/05/$–see front matter
doi:10.1016/j.amjcard.2004.11.040

TABLE 1 Baseline Characteristics

Variable	Low Voltage: Present (n = 35)	Low Voltage: Absent (n = 158)	p Value
Age (yrs)	70 ± 12	67 ± 10	0.124
Men/women	14/21	69/89	0.835
Body mass index (kg/m^2)	21.5 ± 3.2	22.3 ± 4.1	0.280
Albumin (g/L)	35.1 ± 4.3	40.1 ± 3.2	<0.001
Globulin (g/L)	26.3 ± 6.6	27.1 ± 5.8	0.473
Total protein (g/L)	61.5 ± 8.7	67.2 ± 6.4	<0.001
Colloid osmotic pressure (mm Hg)	21 ± 4	24 ± 3	<0.001
Hematocrit (%)	36.2 ± 4.3	37.7 ± 4.6	0.078

TABLE 2 Echocardiographic Indexes

Variable	Low Voltage: Present (n = 35)	Low Voltage: Absent (n = 158)	p Value
Left ventricular			
Ejection fraction (%)	70 ± 7	70 ± 7	1.000
Diastolic dimension (mm)	43 ± 5	44 ± 4	0.204
Systolic dimension (mm)	26 ± 4	27 ± 4	0.182
Ventricular septum (mm)	9.5 ± 1.1	9.3 ± 1.1	0.332
Posterior wall (mm)	9.5 ± 1.4	9.2 ± 1.1	0.168
Left atrium (mm)	33 ± 5	34 ± 5	0.286

diographic abnormalities. Patients with pericardial effusion or anasarca were not included in this study.

Electrocardiograms were obtained within 24 hours of echocardiography, and R- and S-wave amplitudes were measured directly from the standard 12-lead electrocardiograph to the nearest 0.5 mm using calipers and a magnifying glass. The average of 3 QRS complexes (sum of R and S waves) was determined for each lead. Low voltage was defined as a QRS amplitude <5 mm in all limb leads and/or a QRS amplitude <10 mm in all precordial leads. Low voltage was considered present only after diagnosis by 2 cardiologists who had no knowledge of clinical findings. For patients with low voltage, total QRS wave amplitude was defined as the sum of the R- and S-wave amplitudes in 6 limb leads.

Blood samples were taken within <24 hours of the electrocardiogram. Serum albumin was measured by dye-binding bromcresol green procedure and total protein by the Biuret method using a Hitachi 747 analyzer (Hitachi, Tokyo, Japan). Hypoalbuminemia was defined as <38 g/dl. Colloid osmotic pressure was calculated according to the equation by Nitta et al[8] and Staub et al,[9]: [Colloid osmotic pressure = $a(2.8c + 0.18c^2 + 0.012c^3) + b(0.9c + 0.12c^2 + 0.004c^3)$], where "a" is the albumin fraction, "b" is the globulin fraction, and "c" is total protein (grams per liter). Hematocrit was measured by the red blood cell cumulative pulse height detection method using the Sysmex SE 9000 hematology analyser (Sysmex, Kobe, Japan).

An experienced echocardiographer performed M-mode and 2-dimensional echocardiography with a Toshiba SSH 160A phased-array sector scanner

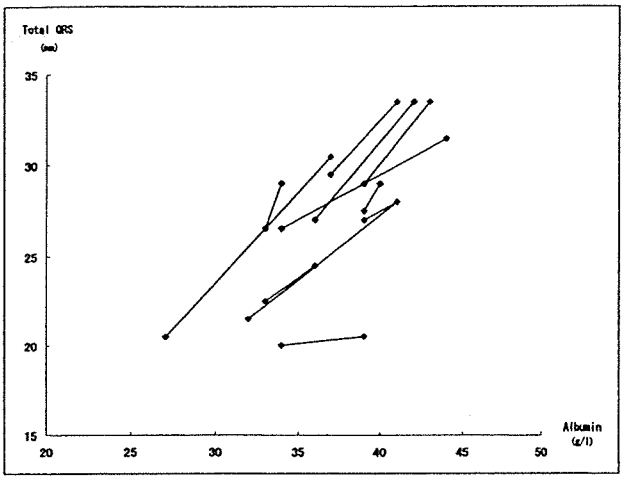

FIGURE 1. Relation of change in total QRS amplitude to change in serum albumin concentration.

(Toshiba, Tokyo, Japan) using a 3.75- or 2.5-MHz transducer. The internal dimension of the left ventricle at end-diastole was measured at the onset of the QRS complex, and the end-systolic dimension was measured at the nadir of septal motion.[10] The thickness of the ventricular septum and posterior wall was measured at the onset of the QRS complex. All classic views were recorded on videotape for subsequent analysis by observers who were unaware of the electrocardiographic data.

Results are reported as mean ± SD. Statistical analysis between the 2 groups was performed by Student's *t* test for continuous variables and Fisher's exact probability test for discrete variables. A paired *t* test was used for paired samples. Regression analysis was used to evaluate the relation between the 2 variables. A p value <0.05 was considered significant.

Among 193 patients, 142 patients were referred to the echocardiographic laboratory to rule out heart disease before operation; 17 patients had connective tissue disease and 34 patients had other noncardiac disorders. Low voltage was detected in 35 patients (18%). Values for albumin and total protein, and colloid osmotic pressure were significantly lower in patients with low voltage compared with those without, but there were no significant differences in the echocardiographic indexes between the 2 groups (Tables 1 and 2). Twenty-seven of 57 patients with hypoalbuminemia had low voltages, whereas 8 of 136 patients without hypoalbuminemia had low voltages. The sensitivity and specificity of low voltages to identify hypoalbuminemia were 47% and 94%, respectively.

In patients with low voltage, there was a fair relation between QRS amplitude and albumin concentration ($r = 0.69$, $p < 0.001$). Follow-up electrocardiography, echocardiography, and serum albumin values were obtained in 11 patients at a mean follow-up of 3.2 ± 2.1 months (0.5 to 6). The serum albumin concentration increased in 9 patients and decreased in 2 patients. Although there were no significant changes in left ventricular diastolic dimension (44 ± 5 vs 44 ± 5 mm), left ventricular systolic dimension (27 ± 6 vs 27 ± 5 mm), septal

thickness (10 ± 1 vs 10 ± 1 mm), and left ventricular posterior wall thickness (10 ± 1 vs 10 ± 1 mm), an increase (decrease) in albumin was accompanied by an increase (decrease) in the total QRS wave amplitude (Figure 1). Moreover, there was a good correlation between the change in total QRS amplitude and the change in albumin concentration ($r = 0.78$, $p = 0.005$).

• • •

The attenuation of QRS wave amplitude is linked to obesity, various lung diseases, and anasarca, whereas augmentation of QRS wave amplitude is associated with a reduction in hematocrit or after hemodialysis.[5–7,11–14] Despite no significant differences in echocardiographic indexes, hematocrit, and body mass index, the serum albumin concentration was significantly lower in patients with low voltages compared with those without. Moreover, low voltage was a highly specific, although not sensitive, electrocardiographic sign of hypoalbuminemia. When the change in albumin concentration and in QRS wave amplitude was assessed, there was a good correlation between these 2 variables. These data indicate that the surface electrocardiographic potentials are attenuated when the resistance of the extracellular space is decreased because of increased extracellular fluid. Thus, serum albumin concentration can affect QRS wave amplitude in patients free of heart and lung diseases.

1. Unverferth DV, Williams TE, Fulkerson PK. Electrocardiographic voltage in pericardial effusion. *Chest* 1979;75:157–160.
2. Spodick DH. The normal and diseased pericardium: current concepts of pericardial physiology, diagnosis and treatment. *J Am Coll Cardiol* 1983;1:240–251.
3. Meyers DG, Bagin RG, Levene JF. Electrocardiographic changes in pericardial effusion. *Chest* 1993;104:1422–1426.
4. Kudo Y, Yamasaki F, Doi T, Doi Y, Sugiura T. Clinical significance of low voltage in asymptomatic patients with pericardial effusion free of heart disease. *Chest* 2003;124:2064–2067.
5. Wagner GS. Marriott's Practical Electrocardiography. 9th Ed. Baltimore: Williams & Wilkins, 1994:176–179.
6. Heaf JG. Albumin-induced changes in the electrocardiographic QRS complex. *Am J Cardiol* 1985;55:1530–1533.
7. Madias JE, Bazaz R, Agarwal H, Win M, Medepalli L. Anasarca-mediated attenuation of the amplitude of electrocardiogram complexes: a description of a heretofore unrecognized phenomenon. *J Am Coll Cardiol* 2001;38:756–764.
8. Nitta S, Ohnuki T, Ohkuda K, Nakada T, Staub NC. The corrected protein equation to estimate plasma colloid osmotic pressure and its development on a nomogram. *Tohoku J Exp Med* 1981;135:43–49.
9. Staub NC. Pathophysiology of pulmonary edema. In: Staub NC, Taylor AE, eds. Edema. New York: Raven Press, 1984:719–746.
10. Henry WL, Gardin JM, Ware JH. Echocardiographic measurements in normal subjects from infancy to old age. *Circulation* 1980;62:1054–1060.
11. Rudy Y, Plonsey R, Liebman J. The effects of variations in conductivity and geometrical parameters on the electrocardiogram, using an eccentric spheres model. *Circ Res* 1979;44:104–111.
12. Rosenthal A, Restieaux NJ, Feig SA. Influence of acute variations in hematocrit on the QRS complex of the Frank electrocardiogram. *Circulation* 1971;44:456–465.
13. Ishikawa K, Nagasawa T, Shimada H. Influence of hemodialysis on electrocardiographic wave forms. *Am Heart J* 1979;97:5–11.
14. Dudley SC, Baumgarten CM, Ornato JP. Reversal of low voltage and infarction pattern of the surface electrocardiogram after renal hemodialysis for pulmonary edema. *J Electrocardiol* 1990;23:341–345.

Original Paper

nephron
Experimental
Nephrology

Nephron Exp Nephrol 2005;100:e95–e103
DOI: 10.1159/000084575

Received: August 31, 2004
Accepted: December 8, 2004
Published online: March 17, 2005

Hypoxia-Inducible Factor-1α Is Involved in the Attenuation of Experimentally Induced Rat Glomerulonephritis

Yoshihiro Kudo[a] Yoshihiko Kakinuma[b] Yasukiyo Mori[e]
Norihito Morimoto[a] Takashi Karashima[c] Mutsuo Furihata[d]
Takayuki Sato[b] Taro Shuin[c] Tetsuro Sugiura[a]

Departments of [a]Laboratory Medicine, [b]Cardiovascular Control, [c]Urology and [d]Tumor Pathology, Kochi Medical School, Kochi, and [e]The Second Department of Internal Medicine, Kansai Medical University, Osaka, Japan

Key Words
Glomerulonephritis · Habu snake venom · Angiotensin II · Hypoxia-inducible factor-1α

Abstract
Background/Aim: Among various kidney disease models, there are few rat glomerulonephritis (GN) models that develop in a short time, and with mainly glomerular lesions. Hypoxia-inducible factor (HIF)-1α is a transcriptional factor that induces genes supporting cell survival, but the involvement of HIF-1α in attenuating the progression of GN remains to be elucidated. We developed a new model of rat GN by coadministration of angiotensin II (AII) with Habu snake venom (HV) and investigated whether HIF-1α is involved in renal protection. ***Methods:*** Male Wistar rats were unilaterally nephrectomized on day 1, and divided into 4 groups on day 0; N group (no treatment), HV group, A group (AII), and H+A group (HV and AII). To preinduce HIF-1α, cobalt chloride ($CoCl_2$) was injected twice before injections of HV and AII in 11 rats. ***Results:*** GN was detected only in the H+A group; observed first on day 2 and aggravated thereafter. HIF-1α was expressed in the glomeruli and renal tubules in the A and H+A groups. In the H+A group, GN was remarkably reduced by $CoCl_2$ pretreatment (44.9 to 12.2%, $p < 0.01$). ***Conclusion:*** Both HV and AII were critical for the development of GN, and HIF-1α remarkably attenuated the progression of GN.

Introduction

Many animal studies have been performed in attempts to overcome the poor prognosis of chronic renal failure due to diabetic nephropathy and glomerulonephritis (GN) [1–5]. Although factors involved in the pathogenesis of GN have been intensively investigated, the development of a proper animal GN model with high reproducibility and simplicity as well as a model without time-consuming process is required. Experimental rat models of GN are classified into several groups in terms of the pathophysiological mechanisms of renal diseases. Anti-glomerular basement membrane nephritis was developed with depositions of immune complex using anti-glomerular basement membrane antibody [3, 6], tubulointerstitial injury was caused by cyclosporine A [4] and injury of renal tubules by ischemia [5]. However, there are few rat GN models with mainly pathological features in the glo-

KARGER
Fax + 41 61 306 12 34
E-Mail karger@karger.ch
www.karger.com

1660–2129/05/1002–0095$22.00/0

Accessible online at:
www.karger.com/nee

Yoshihiko Kakinuma, MD, PhD
Department of Cardiovascular Control
Kochi Medical School
Nankoku, Kochi 783-8505 (Japan)
Tel. +81 88 880 2311, Fax +81 88 880 2310, E-Mail kakinuma@med.kochi-u.ac.jp

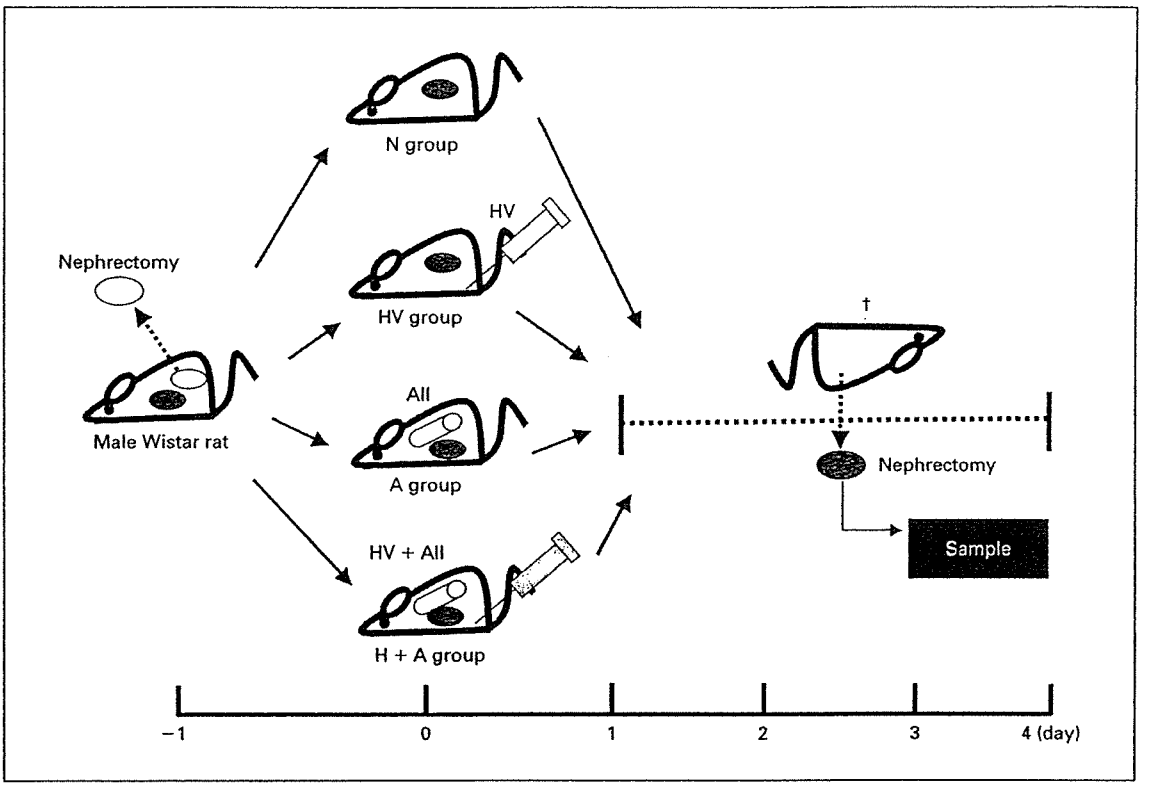

Fig. 1. Study Protocol. All rats are unilaterally nephrectomized on day 1 and divided into 4 groups on day 0. N group: no injection of reagents. HV group: injection of 3.5 mg/kg of Habu snake venom (HV). A group: continuous administration of 100 ng/min of angiotensin II (AII). H+A group: administration of HV and AII.

meruli that are developed in a short time [7]. Angiotensin II (AII) is known to increase blood pressure through vascular contraction, and to be profoundly involved in cardiovascular hypertrophy and the contraction of intrarenal arteries. AII is also directly involved in the progression of glomerulosclerosis via the effect of hyperfiltration with or without hypertension [8, 9]. Many studies have revealed important factors involved in the pathogenesis of GN or factors aggravating GN, but evaluating further factors that suppress the occurrence of GN is also crucial. To investigate the features of renal protection, we focused on hypoxia-inducible factor (HIF)-1α. HIF-1α, a transcriptional factor with formation of a heterodimer with HIF-1β [10], is post-transcriptionally regulated and its protein level is elevated by hypoxia through inhibition of ubiquitin-mediated degradation. HIF-1α is known to be a survival factor responsible for inducing lines of genes supporting cell survival such as glucose metabolism (glucose transporters and glycolytic enzymes), vasomotor regulation (heme oxygenase-1 and endothelin-1), angiogenic growth (vascular endothelial growth factor), and anemia control (erythropoietin and transferrin) [11–13]. Recent studies have demonstrated that non-hypoxic stimuli like AII can also activate HIF-1α [14, 15], but the role of HIF-1α induction in attenuating the progression of GN remains to be elucidated. Accordingly, we developed a new rat GN model by coadministration of AII with Habu snake venom (HV) and investigated whether preinduction of HIF-1α leads to renal protection.

Materials and Methods

Development of Rat GN Model

All experiments were approved by the institutional review board for the care of animal subjects and were performed in accordance with guidelines of Kochi Medical School. Nine-week-old male Wistar rats (180–220 g) were purchased from Japan SLC (Shizuoka, Japan). Rats were unilaterally nephrectomized on day 1. On day 0, the rats were divided into 4 groups. In the first group, no treatment was performed with any reagents or surgical procedure (N group, n = 6). In the second group, rats were injected with 3.5 mg/kg of HV (Sigma-Aldrich Co., Steinheim, Germany) through the femoral vein (HV group, n = 11). In the third group, rats were continuously adminis-

tered with AII (100 ng/min; Peptide Institute Inc., Osaka, Japan) using Alzet osmotic pumps (DURECT Co., Cupertino, Calif., USA) (A group, n = 11). In the fourth group, rats were administered with both HV and AII (H+A group, n = 22). Rats were sacrificed on day 1, 2, 3 or 4, and kidneys excised for histochemical analysis (fig. 1).

Measurement of Systolic Blood Pressure

Systolic blood pressure (SBP) was measured by the tail-cuff method with an electro-sphygmomanometer (BP-98A; Softron Co., Tokyo, Japan). SBP was measured in conscious rats every day from day 1 to 2. The SBP value for each rat was calculated as the average of 3 separate measurements at each session. SBP measurement was performed between 9 and 12 a.m. by a single blinded investigator.

Measurements of Serum Urea Nitrogen and Creatinine

Before the sacrifice, blood samples were obtained via an axillary vein for determination of serum urea nitrogen (UN) and creatinine (Cr) levels. Serum UN and Cr levels were determined enzymatically with automation-analysis equipment (Hitachi 7350; Hitachi Co., Ibaragi, Japan) in our laboratory center.

Histological Analysis

To evaluate the progression of GN in our animal model, histological analyses were performed using the periodic acid-Schiff (PAS) and periodic acid-methenamine silver (PAM) reagents. After the specimens were paraffin embedded, 4-μm-sectioned samples were stained with PAS and PAM reagents and counterstained with hematoxylin. For quantitative analysis, the ratio of damaged glomeruli to all glomeruli in the sectioned sample was calculated and the percentage of GN in the section was evaluated. Moreover, semiquantitative analysis was performed to evaluate more precisely the morphological changes of our GN model according to the protocol in previous studies [16, 17]. A minimum of 20 glomeruli (ranging from 20 to 60 glomeruli) in each specimen were examined and the severity of the mesangiolysis lesion was graded from 0 to 4+ according to the percentage of glomerular involvement; a 1+ lesion represented an involvement of 25% of the glomerulus while a 4+ lesion indicated that 100% of the glomerulus was involved. Thus, the mesangiolysis score (MES) was then obtained by multiplying the degree of damage (0 to 4+) by the percentage of the glomeruli with the lesion. Tubular injuries including tubular necrosis or occlusion of collecting ducts by cast material were graded as mild (1+), moderate (2+), or severe (3+).

Western Blot Analysis

Nuclear protein from whole kidney was prepared using NE-PER Nuclear and Cytoplasmic Extraction Reagents (Pierce Biotechnology Inc., Rockford, Ill., USA). Nuclear protein was electrophoresed using 10% SDS-PAGE gels and transferred to polyvinylidene difluoride membrane (Immobilon-P; Millipore Corp., Bedford, Mass., USA). A monoclonal IgG HIF-1α antibody α67 (Novus Biological, Littleton, Colo., USA) was used; a horseradish peroxidase-conjugated antibody (Promega Co., Madison, Wisc., USA) was used as a secondary antibody. The ECL Western blotting systems (Amersham Bioscience, Uppsala, Sweden) was used for detection.

Immunohistochemical Analysis

Paraffin sections including the samples were dewaxed in xylene and rehydrated in a series of ethanol, and then washed in distilled water before staining procedures. According to the instruction provided by the manufacturer, HIF-1α was identified with rabbit polyclonal anti-HIF-1α antibody H-206 (Santa Cruz Biotechnology, Calif., USA) utilizing the catalyzed signal amplification system (Dako, Hamburg, Germany) based on the streptavidin-biotin-peroxidase reaction. Antigen retrieval was performed for 5 min in a preheated Dako target retrieval solution using a microwave. Incubation procedures were performed in a humidified chamber. Following the incubation, specimens were washed 3 times in TBST buffer. The specificity of staining was confirmed by substitution of the primary antibody for a normal rabbit IgG and additionally by an immunohistochemical reaction without a primary antibody but with the secondary antibody alone.

An Experiment Using Cobalt Chloride as a Pretreatment

Rats were twice subcutaneously administered 30 mg/kg of cobalt chloride ($CoCl_2$) at a 12-hour interval ($CoCl_2$ group) (n = 11), followed by unilateral nephrectomy. Then, the rats were administered with HV and AII. As a comparison, rats were injected with 0.9% NaCl solution instead of $CoCl_2$, followed by the same protocol as the $CoCl_2$ group (n = 11). After $CoCl_2$ administration, however, before injection of HV and AII, a kidney was excised as a sample to examine expression level of HIF-1α ($CoCl_2$ Pre). Likewise, 2 days after administration of HV and AII, a kidney was also excised ($CoCl_2$ Day 2). To compare the expression level of HIF-1α by $CoCl_2$ before GN and the severity of pathology of GN, we investigated whether preinduction of HIF-1α is involved in renal protection.

Statistical Analysis

Data are reported as mean ± SEM. A paired t test was used for paired samples and Student's t test was used to compare the 2 groups. One-way layout analysis of variance or repeated measures of analysis of variance were used to compare multiple groups. If the p value was significant, Scheffé's multiple comparison was performed. A p value <0.05 was considered significant.

Results

AII Combined with HV Developed GN

Morphological studies using PAS and PAM staining revealed that there are no glomerular or tubular injuries in N group (fig. 2a), HV group (fig. 2b), A group (fig. 2c), however, GN was detected only in the H+A group (fig. 2e). Although renal tubular casts were observed, glomerular changes were scarcely observed on day 1 after AII and HV administration (fig. 2d, 3). GN was initially detected on day 2 (fig. 2e, f, 3), followed by further aggravation during the time course (data not shown). Renal tubular injury including tubular necrosis was not remarkable, and extensive cellular infiltration was not found in the interstitial regions (fig. 3). On the other hand, characteristic focal and segmental mesangiolysis, explained as capillary aneurysmal ballooning, was observed with dilatation of glomerulus (fig. 2e, f). The rate of occurrence of GN on day 2 was 44.9 ± 2.6%, and the MES score of the H+A

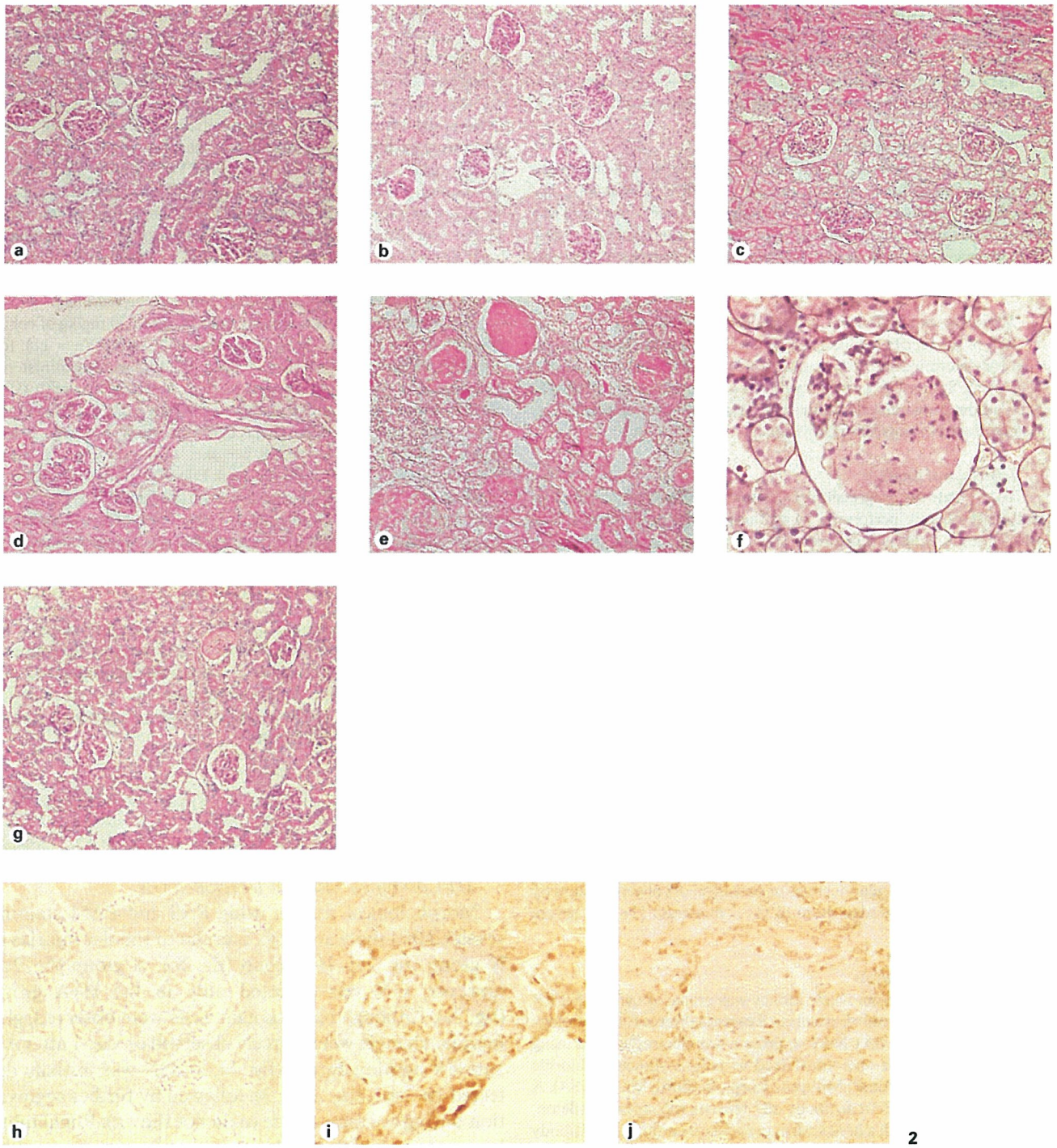

2

group was 199 ± 15 (fig. 3). On the other hand, in the HV group, less than 2% had morphologic changes of mesangiolysis during 4 days, and the MES score was 10 ± 5 (fig. 2b, 3). Moreover, in the A group, there were no morphologic changes during the time course (fig. 2c).

Changes in Serum UN and Cr

Serum UN and Cr were 18.4 ± 0.7 and 0.31 ± 0.01 mg/dl, respectively, on day 2 in the N group. In the H+A group, serum UN and Cr levels increased to 41.5 ± 4.0 and 0.57 ± 0.05 mg/dl, respectively, on day 2; significantly higher than those in the N group (fig. 4a, b). In contrast, serum UN and Cr levels in the H+A group on day 1 (24.0 ± 1.8 and 0.42 ± 0.02 mg/dl, respectively) were similar to the level of the N group. There were no significant differences in serum UN and Cr level among the HV, A and N groups.

SBP Response

SBP values of each group are shown in figure 4c. There were no significant differences in SBP after nephrectomy among the 4 groups. Administration of AII caused a significant increase of SBP on day 1 (186 ± 4 mm Hg) and persisted to day 2 (192 ± 1 mm Hg). SBP in the H+A group on day 2 (183 ± 3 mm Hg) was comparable to that in the A group. Administration of HV had no influence on SBP during the 2 days.

Expression Level of HIF-1α Protein

Western blot analysis revealed that the expression level of HIF-1α protein increased in the H+A and A groups (fig. 5a), compatible with the results of immunohistochemical analysis. Expressions of HIF-1α protein were observed in the A and H+A groups, but protein expression was not detected in the N and HV groups. These data suggest that HIF-1α was induced mainly by AII, and, at least in part, was related to the pathogenesis of GN or to the defense mechanism against the progression of GN.

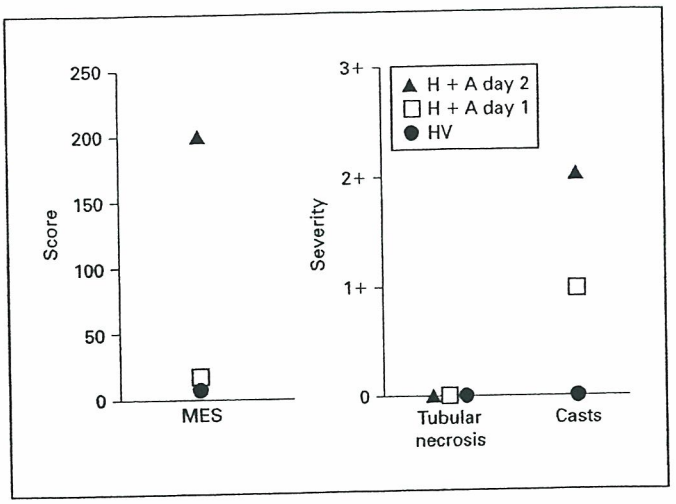

Fig. 3. Semiquantitative analysis of morphologic changes in our glomerulonephritis model. The main lesion in the H+A group is initially detected on day 2 as mesangiolysis in glomeruli; however, there are no tubular lesions of necrosis except for tubular casts; in contrast, there are no morphological changes in the N and A groups. MES = Mesangiolysis score.

Induction of HIF-1α in Glomeruli and Renal Tubules

Immunohistochemical study demonstrated positive nuclear staining of HIF-1α in glomeruli, renal tubules (fig. 2i, j), collecting ducts and epithelium of the papilla (data not shown) in the A and H+A groups. In contrast, no positive nuclear signals were detected in the N (fig. 2h) and HV (data not shown) groups. HIF-1α-positive cells were mainly detected in mesangial cells in glomeruli (fig. 2i, j). As demonstrated, especially in the H+A group (fig. 2j), HIF-1α was expressed in the intact part of the glomerulus, but not in the injured part of the same glomerulus. Furthermore, nuclear HIF-1α-positive signals were observed in smooth muscle cells in peripheral renal arteries (data not shown).

$CoCl_2$ Pretreatment Inhibits the Progression of GN

To further investigate whether HIF-1α is involved in the development of nephropathy or in the antiprogressive action, we pretreated rats with $CoCl_2$. As demonstrated in figure 5b, pretreatment with $CoCl_2$ increased HIF-1α expression before administration of HV and AII (Pre-1),

Fig. 2. Glomerulonephritis is developed with the combination of HV and AII, and HIF-1α is induced in the intact glomeruli. There are no glomerular or tubular injuries in N group (**a**), HV group (**b**), A group (**c**) and H+A group on day 1 (**d**). Damaged glomeruli, characterized by extensive mesangiolysis, are observed in H+A group on day 2. PAS staining. Magnification, ×100 (**e**). Focal and segmental mesangiolysis with large capillary aneurysmal ballooning are observed in the H+A group on day 2. PAM staining. Magnification, ×400 (**f**). The number of GN was significantly less in pretreatment with $CoCl_2$ than without. PAS staining. Magnification, ×100 (**g**). Immunoreactive HIF-1α-positive signals are not detected in the N group (**h**). Nuclear HIF-1α signals are observed in a glomerulus and tubules in the A group. Magnification, ×200 (**i**). A glomerulus in the H+A group on day 2 possesses intact cells with HIF-1α-positive signals; in contrast, other parts have few HIF-1α signals due to mesangiolysis. Magnification, ×200 (**j**).

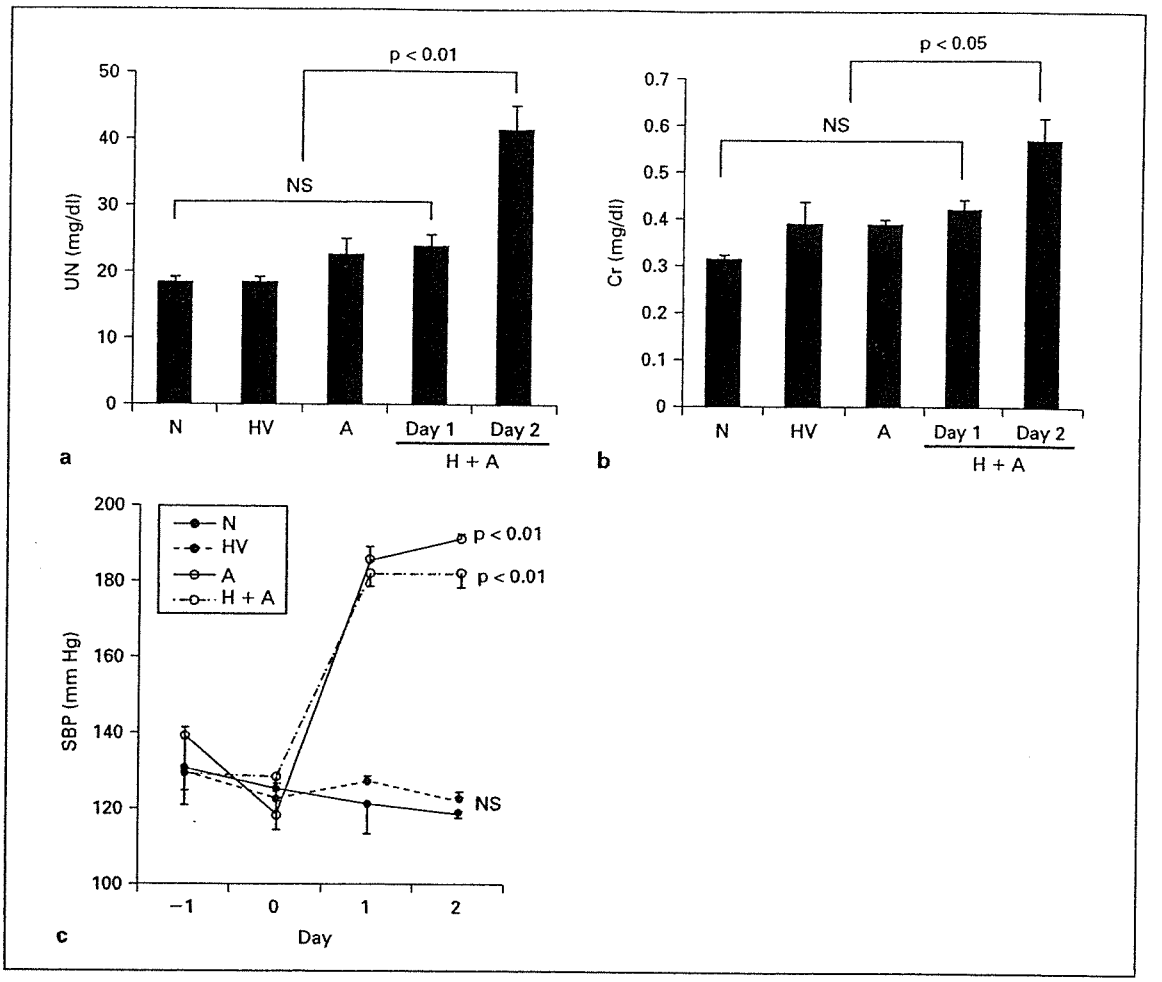

Fig. 4. Serum UN, Cr and SBP are increased with the combination of HV and AII. The serum UN (**a**) and Cr (**b**) levels in the H+A group on day 2 are significantly higher than other groups. SBP increases significantly with administration of AII (A and H+A groups) (**c**).

suggesting that HIF-1α was induced by $CoCl_2$ before development of GN. Even on day 2, the expression level of HIF-1α was increased in the $CoCl_2$ group ($CoCl_2$ Day 2-1). In the $CoCl_2$ group, focal mesangiolysis with glomeruli enlargement was still observed, but the number of GN was much less than in those without $CoCl_2$ pretreatment (fig. 2g).

Thus, 7 of 11 rats (63.6%) with $CoCl_2$ pretreatment were rescued from GN alone, while the other 4 (36.4%) were not; showing a comparable severity level of GN with the non-$CoCl_2$ group. As demonstrated in figure 5b, unlike Pre-1, Pre-2 did not induce HIF-1α with $CoCl_2$ and showed no $CoCl_2$ suppression of GN. The ratio between rats rescued or not rescued from GN was comparable with that between preinduction and noninduction of HIF-1α by $CoCl_2$, as demonstrated in figure 5c. In the $CoCl_2$ group, the rate of GN from each rat decreased to 12.2 ± 2.1%, which was in great contrast to 44.9 ± 2.6% in the non-$CoCl_2$ group. Furthermore, serum UN and Cr levels on day 2 were significantly lower in the $CoCl_2$ than in the non-$CoCl_2$ group ($p < 0.05$) (fig. 6a, b), despite comparable SBP values between the 2 groups (fig. 6c).

Discussion

In this study, we developed a new model of GN induced by both HV and AII. This model has several distinct characteristics. First, GN developed rapidly, and was detected on the second day after administration of

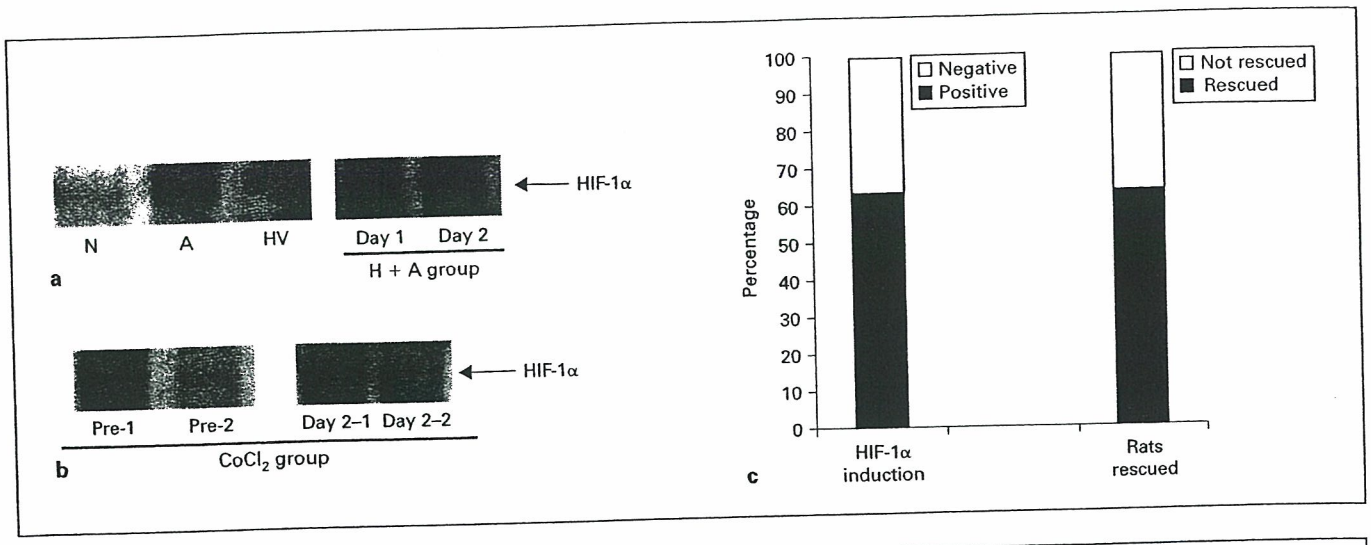

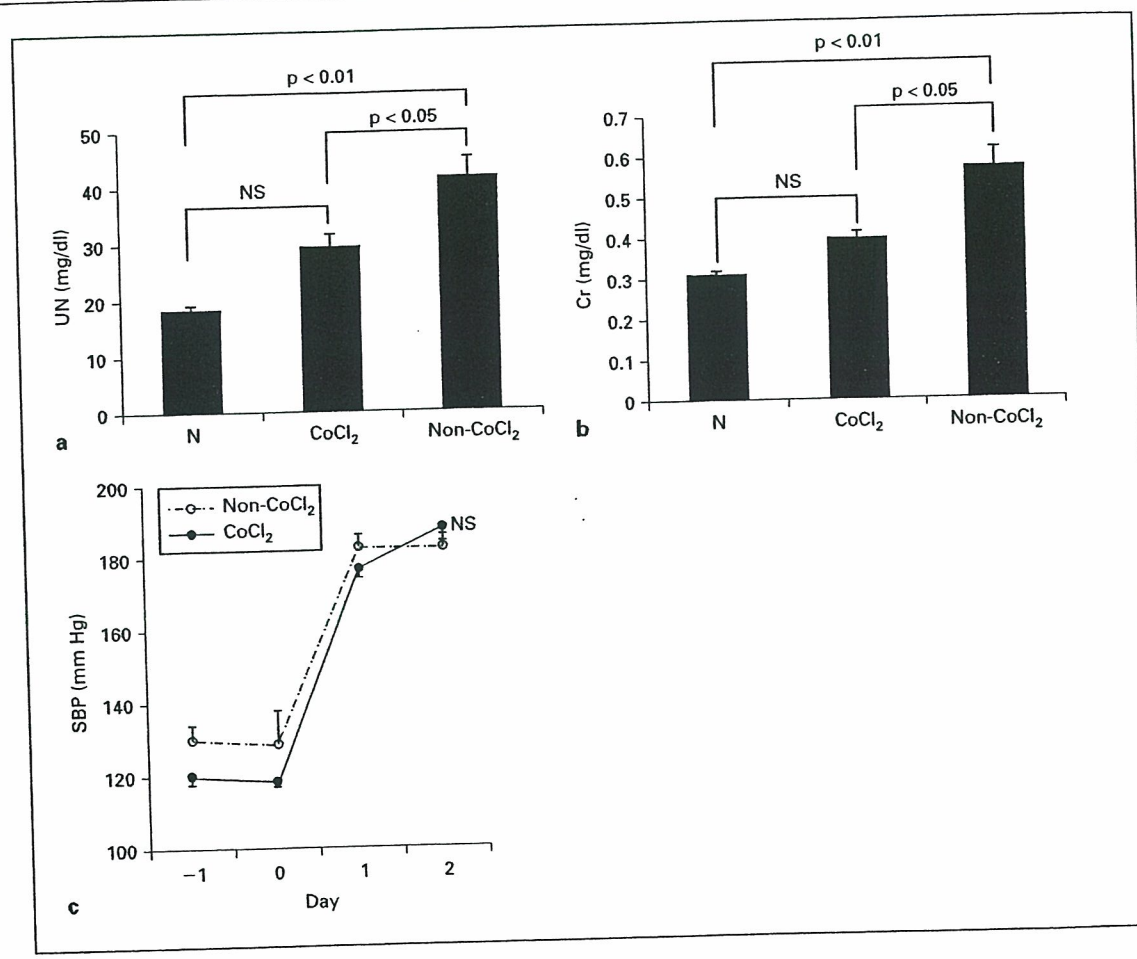

Fig. 5. The protein level of HIF-1α is increased by administration of HV and AII, and pretreatment of $CoCl_2$ increases HIF-1α expression before development of GN. HIF-1α is not detected in the N and HV groups (Day 2). However, HIF-1α is detected in A (Day 2) and H+A (Days 1 and 2) groups (**a**). The $CoCl_2$ group, in accord with the level of HIF-1α induction, was divided into 2 groups. HIF-1α is greatly induced before the development of GN ($CoCl_2$ group Pre-1), and is followed by a high level ($CoCl_2$ group Day 2-1); in contrast, it is not efficiently induced ($CoCl_2$ group Pre-2), and also is scarcely detected on day 2 ($CoCl_2$ group Day 2-2) (**b**). The rate of preinduction of HIF-1α by $CoCl_2$ is comparable with that of the inhibition of GN by $CoCl_2$ (**c**).

Fig. 6. Pretreatment with $CoCl_2$ attenuates GN. Serum UN (**a**) and Cr (**b**) levels in the $CoCl_2$ group on day 2 are significantly decreased compared to those in the non-$CoCl_2$ group. There is no significant difference in SBP between the $CoCl_2$ and non-$CoCl_2$ groups (**c**).

HV and AII. Many models of GN have been reported including 5/6 nephrectomized and Thy-1.1 nephritis models [18, 19]. However, these models take a long time to develop nephropathy. In contrast, our protocol induced GN in 2 days, suggesting that one of the advantages our model has over others is in terms of the time course. Further, pathological findings were restricted to glomerular regions without remarkable tubular or interstitial lesions. Since our GN model developed within 2 days, it also has advantages for disclosing the specifically critical time point of the development of GN. Furthermore, the development rate of GN was almost 100%, indicating the high reproducibility of our model. This basis of the rat model was initially developed by Barnes et al. [20] who reported that the progression of AII-induced renal injury was accelerated by pre-existing injury induced by HV; our model, which now optimizes the reproducibility of GN, is a modification of theirs.

Habu-induced nephropathy was reported to develop within 1 day by a dose of 2.0–4.0 mg/kg HV (in our model 3.5 mg/kg) and the main pathological change was 'mesangiolysis' [21, 22]. However, for reasons we have not as yet ascertained, in our study no rats showed Habu-nephropathy-specific pathological findings during the first week in the HV group. On the other hand, AII is one of the major factors responsible for the pathogenesis of GN, because it remarkably increases glomerular pressure causing hyperfiltration, production of extracellular matrix and expression of lines of genes involving GN [23–25]. Further, since AII has some ischemic effects on the kidneys, there is the possibility that an AII-induced ischemic effect causes the GN depicted in our model. However, as demonstrated in this study, glomerular injury was predominantly observed, and was not associated with renal tubular lesions, i.e. tubular necrosis suggesting renal ischemia. Therefore, in accordance with the pathological characteristic of this GN, AII-induced renal ischemia may not be responsible for its development in our model. Additionally, in this study, SBP increased in the A and H+A groups, but GN was not induced in the A group. Therefore, GN in our model was induced not by HV or AII alone, but by the combination of HV and AII, independent of any increase in systemic blood pressure.

HIF-1α is a master transcriptional factor, transactivating the expression of many genes important for cell survival under hypoxic conditions [11–13, 26]. These genes are responsible for glycolysis, angiogenesis, proliferation and iron metabolism, all of which are induced by hypoxic stress; thus, the induction of HIF-1α is a marker of hypoxia. HIF-1α is regulated at the post-translational level by the proteasome system through ubiquitination with von Hippel-Lindau (VHL) protein [27, 28]. As previously reported, this regulation of HIF-1α protein level is dependent on the concentration of oxygen. Hypoxia induces enhancement of HIF-1α protein stability leading to the elevation of the protein level due to inhibition of degradation by VHL. Therefore, hypoxia induces adaptation in cells including induction of HIF-1α; the hypoxic pathway. On the other hand, a line of evidence recently accumulated suggests that HIF-1α is also regulated independently of oxygen concentration through the nonhypoxic pathway [14, 15]. AII is reported to regulate HIF-1α both at transcriptional and post-translational levels in vascular smooth muscle cells cultured under normoxic condition through the AII type 1 receptor [14, 15]. Moreover, HIF-1α is also post-translationally regulated in several cell lines in the presence of tumor necrosis factor-α or nitric oxide independent of oxygen contents [29, 30].

As demonstrated in this study, immunoreactivity of HIF-1α was not detected in the N group (no treatment group), but HIF-1α was detected in the nuclei of glomerular, tubular and epithelial cells of the papilla by administration of AII alone or AII and HV together. This is the first evidence showing that HIF-1α was detected in the kidney by AII, independent of systemic hypoxic stress. As indicated here, HIF-1α was found to be expressed only in intact, not damaged glomeruli. Even within a glomerulus, only the intact part of glomerular cells expressed HIF-1α. Considering the fact that induction of HIF-1α is one of the defense mechanisms for cell survival [31–33], our data indicate that induction of HIF-1α is a marker of glomeruli survival; indeed, it could be a marker of renal protection.

To further investigate whether HIF-1α is involved in the progression or protection of GN, preinduction of HIF-1α was performed with $CoCl_2$ before administration of HV and AII. Surprisingly, the induction of HIF-1α by $CoCl_2$ pretreatment attenuated the progression of GN; the level of GN was reduced from 44.9 to 12.2% and the incidence of GN was reduced from 100 to 36.4%. Furthermore, as indicated, the preinduction of HIF-1α actually affects the inhibition of GN, because the rate of HIF-1α induction was parallel with that of the attenuation of GN. Therefore, our data suggest that HIF-1α is involved, at least in part, in the defense mechanism against the progression of GN, and hence could be a marker for renal protection.

AII is reported to induce HIF-1α [14, 15] and plays a partial role in the renal protective effect; however, the other effects of AII, such as increasing glomerular pressure and modulating gene expression involving in the renal

failure, may overcome any protective effect of AII-induced HIF-1α, and so as a result it may lead to the progression of GN.

In conclusion, we developed a highly reproducible GN model by combining HV and AII. Preinduction of HIF-1α remarkably attenuated the progression of GN, indicating that HIF-1α was involved in the defense mechanism of the kidney.

Acknowledgments

This work was supported by Grants-in-Aid for Scientific Research from the Ministry of Education, Science and Culture (No. 14657409). We thank Dr. Masami Nakatani, Dr. Noriko Kishimoto, Dr. Ichiro Yamasaki, Dr. Yoshitaka Kumon, Dr. Hiroaki Takeuchi, Dr. Jun Imamura, Dr. Mikio Kamioka, Ms. Chiaki Kawada, Ms. Chizuko Sugimoto, and Mr. Takuya Yamaguchi for their helpful advice and generous support.

References

1 Rifai A, Small PA Jr, Teague PO, Ayoub EM: Experimental IgA nephropathy. J Exp Med 1979;150:1161–1173.

2 Ishizaki M, Masuda Y, Fukuda Y, Yamanaka N, Masugi Y, Shichinohe K, Nakama K: Renal lesions in a strain of spontaneously diabetic WBN/Kob rats. Acta Diabetol Lat 1987;24:27–35.

3 Banks KL: Glomerulonephritis, autoimmunity, autoantibody. Animal model: Anti-glomerular basement membrane antibody in horses. Am J Pathol 1979;94:443–446.

4 Elzinga LW, Rosen S, Bennett WM: Dissociation of glomerular filtration rate from tubulointerstitial fibrosis in experimental chronic cyclosporine nephropathy: Role of sodium intake. J Am Soc Nephrol 1993;4:214–221.

5 Arendshorst WJ, Finn WF, Gottschalk CW: Pathogenesis of acute renal failure following temporary renal ischemia in the rat. Circ Res 1975;37:558–568.

6 Wilson CB, Dixon FJ: Immunopathologic mechanisms of renal disease. Ric Clin Lab 1975;5:17–38.

7 Masuda Y, Shimizu A, Mori T, Ishiwata T, Kitamura H, Ohashi R, Ishizaki M, Asano G, Sugisaki Y, Yamanaka N: Vascular endothelial growth factor enhances glomerular capillary repair and accelerates resolution of experimentally induced glomerulonephritis. Am J Pathol 2001;159:599–608.

8 Kim S, Iwao H: Molecular and cellular mechanisms of angiotensin II-mediated cardiovascular and renal diseases. Pharmacol Rev 2000;52:11–34.

9 Lee LK, Meyer TW, Pollock AS, Lovett DH: Endothelial cell injury initiates glomerular sclerosis in the rat remnant kidney. J Clin Invest 1995;96:953–964.

10 Huang LE, Arany Z, Livingston DM, Bunn HF: Activation of hypoxia-inducible transcription factor depends primarily upon redox-sensitive stabilization of its alpha subunit. J Biol Chem 1996;271:32253–32259.

11 Wang, GL, Jiang BH, Rue EA, Semenza GL: Hypoxia-inducible factor 1 is a basic-helix-loop-helix-PAS heterodimer regulated by cellular O_2 tension. Proc Natl Acad Sci USA 1995;92:5510–5514.

12 Rosenberger C, Mandriota S, Jurgensen JS, Wiesener MS, Horstrup JH, Frei U, Ratcliffe PJ, Maxwell PH, Bachmann S, Eckardt KU: Expression of hypoxia-inducible factor-1alpha and -2alpha in hypoxic and ischemic rat kidneys. J Am Soc Nephrol 2002;13:1721–1732.

13 Wenger RH, Rolfs A, Marti HH, Guenet JL, Gassmann M: Nucleotide sequence, chromosomal assignment and mRNA expression of mouse hypoxia-inducible factor-1 alpha. Biochem Biophys Res Commun 1996;223:54–59.

14 Richard DE, Berra E, Pouyssegur J: Nonhypoxic pathway mediates the induction of hypoxia-inducible factor 1alpha in vascular smooth muscle cells. J Biol Chem 2000;275:26765–26771.

15 Page EL, Robitaille GA, Pouyssegur J, Richard DE: Induction of hypoxia-inducible factor-1alpha by transcriptional and translational mechanisms. J Biol Chem 2002;277:48403–48409.

16 Raij L, Azar S, Keane W: Mesangial immune injury, hypertension, and progressive glomerular damage in Dahl rats. Kidney Int 1984;26:137–143.

17 Linas SL, Shanley PF, Whittenburg D, Berger E, Repine JE: Neutrophils accentuate ischemia-reperfusion injury in isolated perfused rat kidneys. Am J Physiol 1988;255:F728–F735.

18 Romero F, Rodriguez-Iturbe B, Parra G, Gonzalez L, Herrera-Acosta J, Tapia E: Mycophenolate mofetil prevents the progressive renal failure induced by 5/6 renal ablation in rats. Kidney Int 1999;55:945–955.

19 Kaneko Y, Shiozawa S, Hora K, Nakazawa K: Glomerulosclerosis develops in Thy-1 nephritis under persistent accumulation of macrophages. Pathol Int 2003;53:507–517.

20 Barnes JL, Lisa MS: Origin of interstitial fibroblasts in an accelerated model of angiotensin II (AII)-induced interstitial fibrosis. J Am Soc Nephrol 2001;12:699A3645.

21 Cattell V, Bradfield JW: Focal mesangial proliferative glomerulonephritis in the rat caused by habu snake venom. A morphologic study. Am J Pathol 1977;87:511–524.

22 Kitamura H, Sugisaki Y, Yamanaka N: Endothelial regeneration during the repair process following Habu-snake venom induced glomerular injury. Virchows Arch 1995;427:195–204.

23 Ruggenenti P: Angiotensin-converting enzyme inhibition and angiotensin II antagonism in nondiabetic chronic nephropathies. Semin Nephrol 2004;24:158–167.

24 Tolins JP, Raij L: Effects of amino acid infusion on renal hemodynamics. Role of endothelium-derived relaxing factor. Hypertension 1991;17:1045–1051.

25 Nakamura T, Obata J, Kimura H, Ohno S, Yoshida Y, Kawachi H, Shimizu F: Blocking angiotensin II ameliorates proteinuria and glomerular lesions in progressive mesangioproliferative glomerulonephritis. Kidney Int 1999;55:877–889.

26 Makino Y, Cao R, Svensson K, Bertilsson G, Asman M, Tanaka H, Cao Y, Berkenstam A, Poellinger L: Inhibitory PAS domain protein is a negative regulator of hypoxia-inducible gene expression. Nature 2001;414:550–554.

27 Neckers LM: aHIF: The missing link between HIF-1 and VHL? J Natl Cancer Inst 1999;91:106–107.

28 Maxwell PH, Wiesener MS, Chang GW, Clifford SC, Vaux EC, Cockman ME, Wykoff CC, Pugh CW, Maher ER, Ratcliffe PJ: The tumour suppressor protein VHL targets hypoxia-inducible factors for oxygen-dependent proteolysis. Nature 1999;399:271–275.

29 Zhou J, Fandrey J, Schumann J, Tiegs G, Brune B: NO and TNF-alpha released from activated macrophages stabilize HIF-1alpha in resting tubular LLC-PK1 cells. Am J Physiol Cell Physiol 2003;284:C439–C446.

30 Sandau KB, Zhou J, Kietzmann T, Brune B: Regulation of the hypoxia-inducible factor 1alpha by the inflammatory mediators nitric oxide and tumor necrosis factor-alpha in contrast to desferroxamine and phenylarsine oxide. J Biol Chem 2001;276:39805–39811.

31 Prass K, Ruscher K, Karsch M, Isaev N, Megow D, Priller J, Scharff A, Dirnagl U, Meisel A: Desferrioxamine induces delayed tolerance against cerebral ischemia in vivo and in vitro. J Cereb Blood Flow Metab 2002;22:520–525.

32 Furuta GT, Turner JR, Taylor CT, Hershberg RM, Comerford K, Narravula S, Podolsky DK, Colgan SP: Hypoxia-inducible factor 1-dependent induction of intestinal trefoil factor protects barrier function during hypoxia. J Exp Med 2001;193:1027–1034.

33 Matsumoto M, Makino Y, Tanaka T, Tanaka H, Ishizaka N, Noiri E, Fujita T, Nangaku M: Induction of renoprotective gene expression by cobalt ameliorates ischemic injury of the kidney in rats. J Am Soc Nephrol 2003;14:1825–1832.